

# A New Flux and Stator Resistance Identifier for AC Drive Systems

R. J. Kerkman, B. J. Seibel, T. M. Rowan, and D. Schlegel  
Allen-Bradley Co., Standard Drives Business, 6400 W. Enterprise Dr.  
P.O. Box 760, Mequon, Wisconsin, U. S. A., 53092

**Abstract-The effect of stator resistance on AC drive performance is analyzed for flux vector and indirect field oriented controllers. A new technique - the back electromagnetic force (BEMF) detector - for reducing the adverse effects of stator resistance on field oriented control is presented and evaluated through simulation and experimental results. The BEMF detector is shown to reduce the impact of the stator resistance and provides a stator resistance estimate. The detector is compatible with most control strategies and with or without position feedback.**

## I. INTRODUCTION

Modern AC drives require the identification of motor parameters, whether high performance field oriented (FO), flux vector (FV), or volts per hertz (V/Hz). In the case of FO and FV drives, all machine parameters of the single phase equivalent circuit may be necessary. The V/Hz controller, however, requires only the stator resistance for improving the starting torque. The field commissioning procedure, which determines the motor parameters and system mechanical parameters, must be compatible with the control. FO controllers, for example, depend on accurate parameter identification to achieve the expected performance [1,2]. FV controllers, however, may rely on average value or base line parameters stored in memory [3,4].

Once commissioned, the controllers typically incorporate an adaptation mechanism to alter the parameters within the control algorithm. Indirect field oriented controllers (IFOC) alter the slip gain, or equivalently the rotor resistance and magnetizing inductance, and the stator resistance. A number of rotor time constant adaptive controllers have appeared in the literature [5,6]. These adaption techniques improved the performance of IFOC and contributed to the acceptance of FOC by the industrial market. The FV and V/Hz controllers, with their sensitivity to stator resistance changes, employ a slip compensation algorithm to maintain their performance at low speed. In comparison to rotor resistance adaptation, stator resistance adaptation has received less consideration.

Recently, however, Habetler, Profumo, Griva, Pastorelli, and Bettini have proposed a combined adaptive strategy for rotor and stator resistance changes [7]. This technique is specific to stator flux (SF) control and segments the identification procedure as a function of operating frequency.

Another approach by Okuyama, Fujimoto, and Fujii adjusts the stator resistance based on the error between the commanded flux current and the feedback component. As indicated in their paper, however, the algorithm is best suited for low frequency operation [8]. Another solution to the corruption of the voltage feedback by the stator resistance has been through reactive power adaptive techniques [9]. However, this approach to rotor resistance adaptation appears sensitive to the corrupting influence of saturation [10]. A fourth approach uses the third harmonic flux for feedback and adaptation [11]. This technique avoids identifying the stator resistance by sensing the open circuit third harmonic flux. In this case, the neutral of the machine is necessary, which limits its usefulness. Finally, Maruyama and Negoro have presented a technique to estimate the stator and rotor resistances through a backward substitution algorithm [12]. This approach, which assumes accurate motor inductances, was not supported with experimental results.

This paper presents a new technique for reducing the effects of stator resistance on the performance of AC drives. The technique - a back electromagnetic force (BEMF) detector - decouples one component of flux from the corrupting effects of the stator resistance, producing an ideal signal for adaptation algorithms. In addition, the quadrature component provides a near instantaneous estimate of the stator resistance. It is applicable throughout the speed range and is compatible with IFOC, FV, and V/Hz controllers. The paper continues with an analysis of the effects of stator resistance on the performance of FV and FO controllers, then demonstrates its effects by considering experimental data, followed by the theory and block diagram for the BEMF detector, and concludes by presenting simulation and experimental results of its implementation.

## II. THE EFFECT OF STATOR RESISTANCE ON CONTROLLERS

### A. FV

One of the first proposals to improve the performance of V/Hz drives evolved from the first principles of field orientation. FV control of induction motors was presented as a control strategy with performance between that of V/Hz and IFOC [3]. The source of commutation is a voltage vector formed by the two axis voltage components of the q-d machine model. Unlike a current regulated controller, FV rarely contains two-axes proportional - integral (PI) current

controllers. The FV controller of Okuyama employed a PI control on the flux component of current and modified the machine's slip to control the torque producing component of the stator current. The great advantage to this particular control is the lack of voltage feedback. Eliminating the voltage feedback reduces the cost, noise, and complexity of the drive.

Fig. 1 shows a block diagram of the control. The flux current ( $I_d^*$ ) regulator contains an automatic current regulator (ACR2, PI) in combination with voltage feedforward incorporating frequency and stator resistance dependent terms. The output represents the d-axis voltage applied to the motor. The q-axis voltage components consist of the stator flux speed and resistance voltages, and a transient term from the PI output of the flux current regulator. Finally, the q-axis current is controlled through the action of the frequency regulator system. A speed error is generated by comparing the commanded velocity to the velocity estimate, which is formed by subtracting the assumed slip from the electrical frequency. The resulting q-axis current command from the automatic speed regulator (ASR) is compared with the q-axis component of the feedback current. The current regulator output (ACR1) establishes the electrical frequency.

A Monte Carlo simulation analyzed the effects of parameter variation for the control of Fig. 1 on the torque, flux, and speed. The machine ratings ranged from 2 to 1250 Hp. The simulation allowed for independent variation of the parameters and combinations of parameters. For example, the effect of stator resistance on torque was examined with the remaining parameters fixed. The results of the simulation are shown in Fig. 2. Reducing the operating frequency shows an increasing sensitivity in the torque due to errors in the value of the stator resistance employed by the control. Thus, as the machine's temperature increases, the ability to deliver the requisite load at low speed or breakaway is thwarted by the divergence between the control and machine stator resistances.

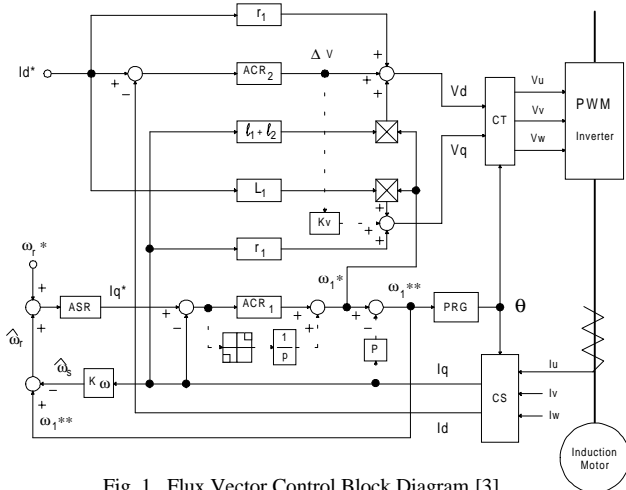


Fig. 1. Flux Vector Control Block Diagram [3].

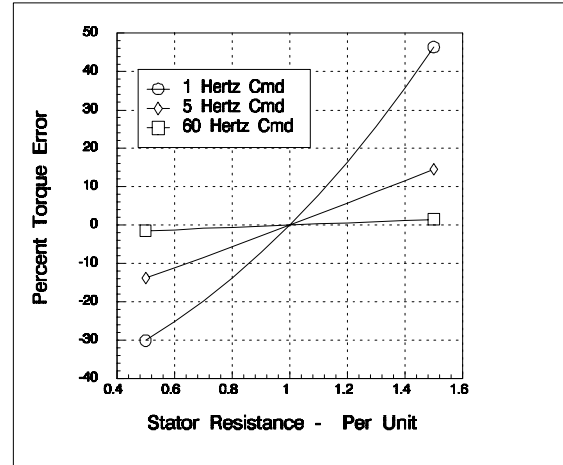


Fig. 2. Torque Error vs Normalized Stator Resistance

Fig. 3 shows the combined effects on torque of simultaneous variations in stator resistance and magnetizing inductance. Fig. 3a displays the results for a 5 Hp machine and Fig. 3b the results for a 500 Hp machine both at 1 Hz electrical equivalent mechanical speed. Comparing the results, the variation in torque with stator resistance and magnetizing inductance can become complex depending on machine size. In contrast to the two dimensional results of Fig. 2, the surfaces of Fig. 3 demonstrate the complex relationship between the control parameters and machine parameters. Low horsepower machines exhibit a nonplanar relationship between the machine's torque and deviations in stator resistance and magnetizing inductance from nominal. As the horsepower increases, the interaction between the stator resistance and magnetizing inductance becomes less pronounced, and reverts to a plane.

Clearly, drive performance would be improved if the control strategy corrected for variations in stator resistance.

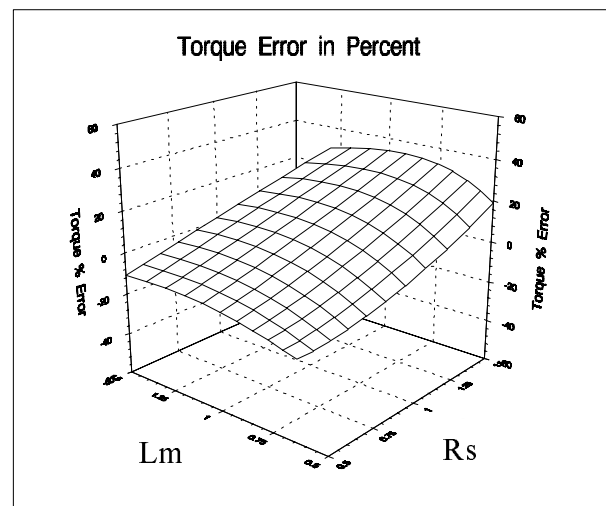


Fig. 3a. Torque Error vs Normalized  $L_m$  and  $r_s$  - 5 Hp Machine at 1 Hz.



and the deviation from zero of the q-axis rotor flux are plotted.

As the stator and rotor resistances increase, the MRAC attempts to correct the slip gain to maintain FO. The simulation shows, however, the compensation is inadequate; the q-axis rotor flux becomes nonzero and the delivered torque exceeds the commanded by approximately 17% at the 4 second point. As the induction machine's temperature increases, the torque increases because the MRAC fails to correctly adjust the slip gain.

Fig. 6 shows experimental results of a current regulated pulse width modulated (CRPWM) IFOC drive system operating at zero speed with full load. The motor was a 4 pole, 460 volt, 10 Hp induction machine. The quantities plotted are the synchronous frame voltages, slip gain, and torque. Over the time interval A, the slip gain is fixed, and no correction is made for changes occurring in rotor resistance. The motor case temperature increases from 26° C to 70° C. As the induction machine's temperature increases, the torque increases by 20%; thus confirming the loss of torque control.

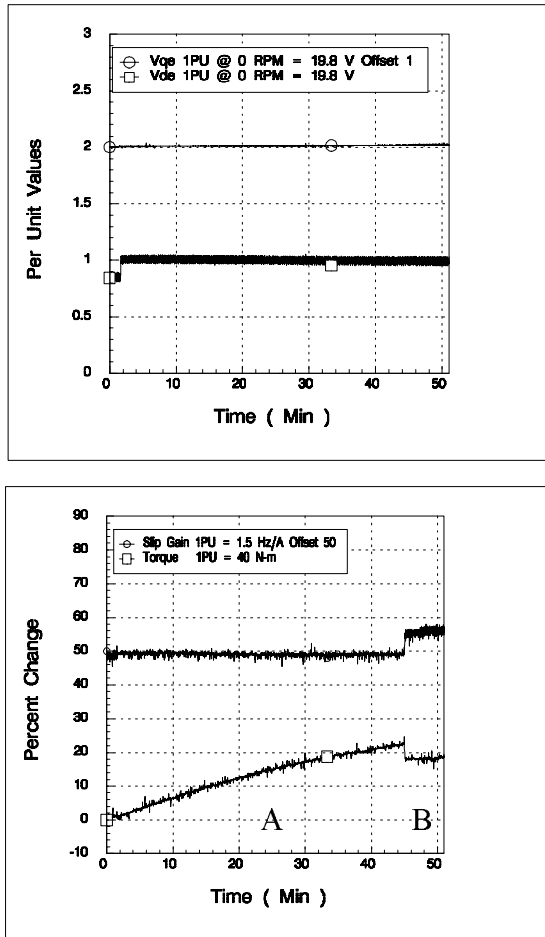


Fig. 6. IFOC Full Load at Zero Speed Demonstrating Heating Effects 10 Hp, 4 Pole, 460 Volt, without and with MRAC - Experimental.

The error in the slip gain degrades FO and the drive reverts to a slip controlled drive system.

Over the time interval B, the MRAC is active; the slip gain, however, fails to adjust sufficiently, even though the MRAC regulates with zero error. This can be explained by referring to the steady state d-axis stator voltage equation (1), when disturbed by small perturbations. As the temperature of the machine increases, the stator and rotor resistances will increase. In the case of the stator resistance, this change may be represented by  $\Delta r_s$ . The effect of the rotor resistance change, however, is not directly measurable, but is observed as a change in the stator flux linkage ( $\Delta \lambda_{qs}$ ). Equation (3) incorporates these effects in the d-axis stator voltage.

$$V_d = (r_s + \Delta r_s) i_d - \omega_e (\lambda_{qs} + \Delta \lambda_{qs}) \quad (3)$$

As the machine's rotor resistance increases, the slip gain is in error, resulting in an increase in the q-axis stator flux. For large values of electrical frequency, the change in q-axis flux dominates and the MRAC corrects for the rotor resistance change by increasing the slip gain. At low frequency, however, the stator resistance change begins to dominate and obscures the flux change; thus, the feedback voltage fails to accurately convey the effects of machine heating. With the stator resistance changing in sympathy with the rotor resistance variation, the d-axis voltage may change slightly, as in Fig. 6, or not at all. With the MRAC inadequately compensating for the change in rotor resistance, the rotor circuits become coupled and FO degrades.

### III. A BEMF DETECTOR AND $R_s$ IDENTIFIER

#### A. Theory

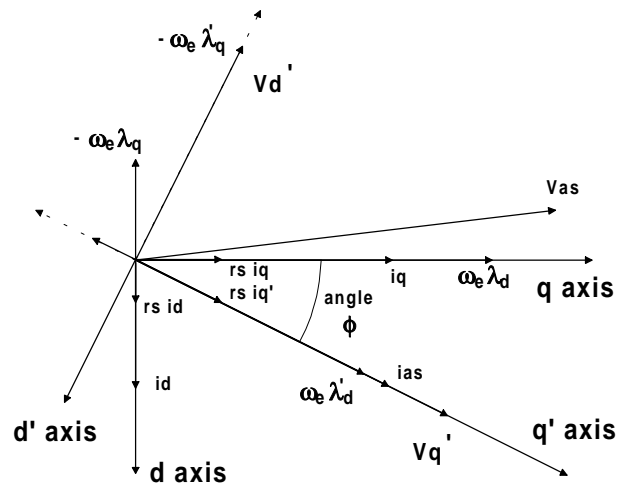


Fig. 7. BEMF Detector and  $R_s$  Identifier Vector Diagram.



rotated by  $\phi$  similar to the feedback voltages (9) and is given by (12).

$$V_d^{*'} = -\omega_e \lambda_q^{*'} \quad (12)$$

where

$$\lambda_q^{*'} = L_\sigma i_q^* \cos(\phi) + \lambda_d^* \sin(\phi) \quad (13)$$

and  $\lambda_d^*$  is the reference field flux.

In the second implementation, Fig. 8b, the BEMF detector is employed as a stator resistance identifier; the output of the identifier updates the value of the stator resistance used in the MRAC. The estimate of the stator resistance is obtained by (14)

$$r_{s_{est}} = (V_q' - \omega_e \lambda_d^{*'}) / i_q^{*'} \quad (14)$$

where

$$\lambda_d^{*'} = \lambda_d^* \cos(\phi) - L_\sigma i_q^* \sin(\phi). \quad (15)$$

This resistance estimate modifies the reference d-axis command voltage as shown in (16).

$$V_d^* = r_{s_{est}} i_d^* - \omega_e L_\sigma i_q^{*'} \quad (16)$$

#### IV. SIMULATION RESULTS

The BEMF detector and stator resistance identifier of the previous section were combined with the MRAC of reference [5]. Both configurations were investigated. Results for the first implementation, Fig. 8a, correspond to FO with encoder feedback. Results for the implementation of Fig. 8b correspond to sensorless FO.

The complexity of a simulation depends on the problem investigated. For minor loop control, a fundamental component model of the system is adequate. Thus, the simulation results shown correspond to fundamental component models for the system elements.

Fig. 9a shows the results of the BEMF detector (Fig. 8a) for conditions identical to Fig. 5. The error in the stator and rotor resistances is displayed in Fig. 9b. An estimate of the rotor resistance may be computed through (6) as described by (17).

$$r_{r_{est}} = \frac{K_s}{K_{s_{FC}}} r_{r_{FC}} \quad (17)$$

With the BEMF detector, the MRAC corrects for the rotor resistance change and maintains the torque within 0.5% of commanded. The q-axis rotor flux is very close to zero and the stator and rotor resistance estimators demonstrate rapid identification. As the resistances increase, the resistance estimators lock within 0.3% and indicate excellent transient tracking characteristics.

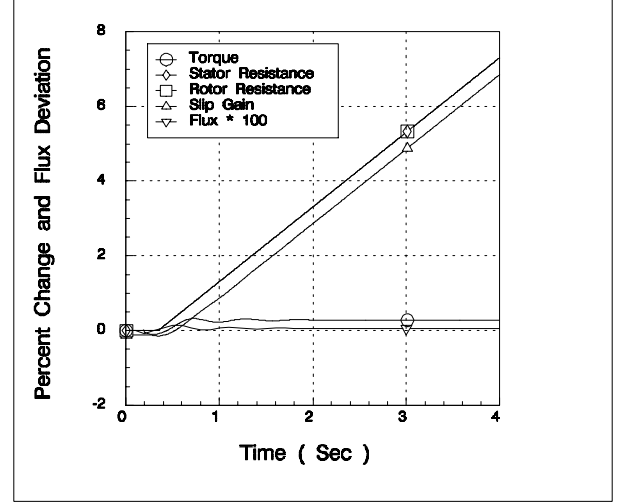


Fig. 9a. IFOC-MRAC with BEMF Detector of Fig. 8a - Simulation.

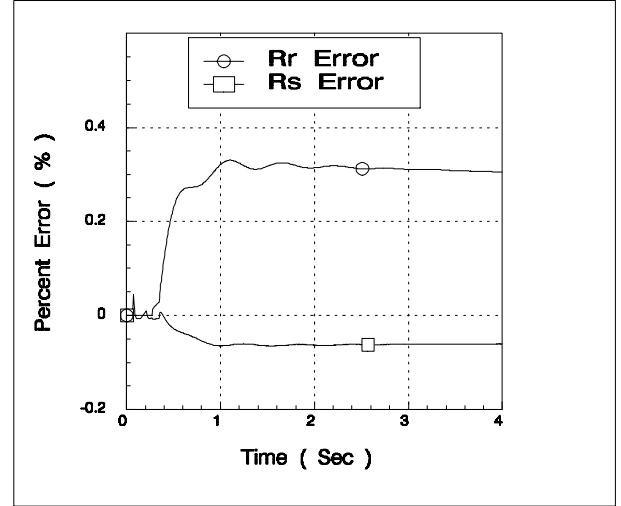


Fig. 9b. IFOC-MRAC with BEMF Detector of Fig. 8a Error in Stator and Rotor Resistances - Simulation.

The results shown in Fig. 10 correspond to the implementation of Fig. 8b and a sensorless FOC. The motor is controlled at 30 rpm with full load applied. In this case, however, the stator resistance suddenly doubles in amplitude. The torque is undisturbed with only a slight deviation in the q-axis rotor flux; demonstrating the BEMF detector's capabilities. In addition, the quadrature component of the detector provides a rapid estimate of the stator resistance.

The MRAC with BEMF detector demonstrates a control with excellent tracking characteristics; one capable of tracking the machine's resistances and correcting the slip gain. By employing an MRAC to adjust the slip gain for rotor resistance variation and incorporating the BEMF detector to remove the corrupting effects of the stator resistance, a simple adaptation method is accomplished.

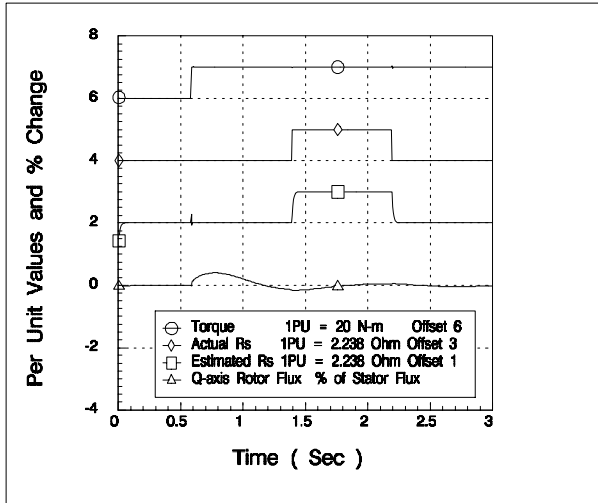


Fig. 10. Sensorless IFOC with BEMF Detector of Fig. 8b Step Change in Stator Resistance at 30 rpm - Simulation.

### V. EXPERIMENTAL RESULTS

The BEMF detectors of Fig. 8 were incorporated with a MRAC based IFOC. The entire control was implemented in an Intel 80196 processor. An analog synchronous regulator with ramp comparison PWM performed the current regulation. The PWM carrier frequency was selectable and the results presented herein were obtained with a 12 kHz carrier. Terminal voltage feedback was provided by a voltage divide down circuit. The feedback voltages were transformed through a 3 to 2 phase conversion followed by a rotation to the synchronous frame.

Fig. 11 shows comparable conditions to those of Fig. 6. The top trace is the slip gain,  $K_s$ . The second trace is the shaft torque obtained from a torque transducer. The third and fourth traces are the synchronous frame machine voltages.

With the drive system at zero mechanical speed and 1 per unit torque command, the MRAC of Fig. 4 is initially inactive - the slip gain ( $K_s$ ) is held constant. The 20 Hp motor case temperature rises from an ambient of 28 C° with 82 N-m of torque to 77 C° and 95 N-m of torque over the interval A - a 16% change. At the beginning of interval B, the MRAC of Fig. 4 is activated with the BEMF detector of Fig. 8a inactive -  $\phi$  is set to zero. Notice the MRAC, even though it regulates to zero error, has little effect on the torque. In fact, the slip gain actually decreases even though the machine's case temperature is increasing. This is not surprising when we look at the response of the d-axis terminal voltage: Throughout interval A, the d-axis voltage barely deviates from the ambient value. This agrees with the description of the effects of stator and rotor heating provided in section II and described by (3).

At the beginning of interval C, the case temperature was 85° C and the torque was 98 N-m; a 20% change in the

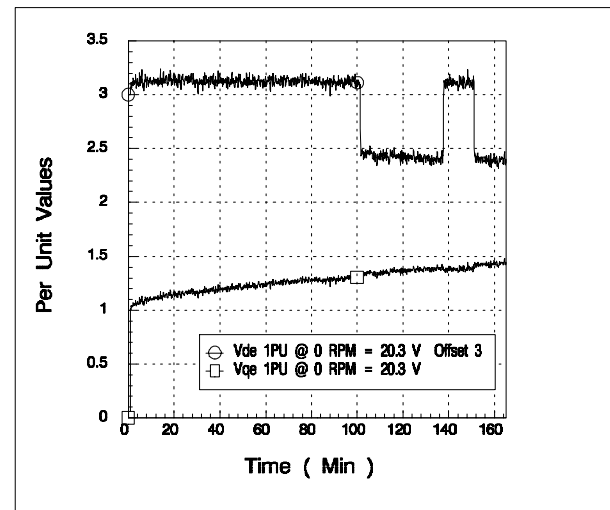
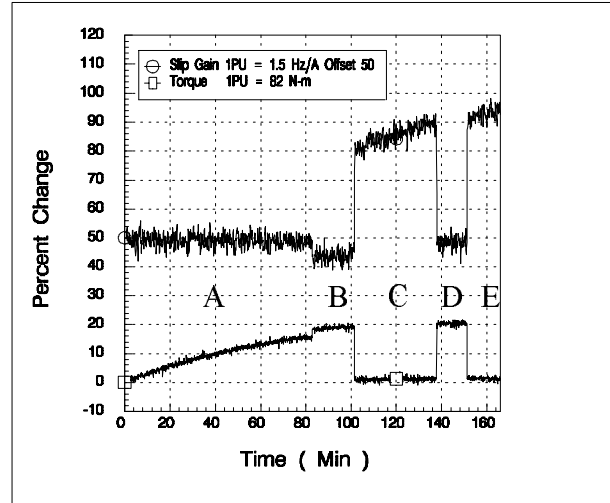


Fig. 11. Sensor IFOC with BEMF Detector of Fig. 8a - Experimental.

delivered torque. At this point, the BEMF detector is activated -  $\phi$  is nonzero. Now the MRAC in conjunction with the output of the BEMF detector corrects for the accumulated effects of stator and rotor resistance heating and adjusts the slip gain to resume FO. The behavior of the terminal voltages are also instructive. Once the BEMF detector is activated, the d-axis voltage becomes the d'-axis voltage and shows a constant level even as the motor continues to heat to 100° C. The torque immediately returns to 81 N-m, very close to the original 82 N-m.

Over intervals D and E, the BEMF detector is alternately switched off and on showing the consistent operation of the control. All the while, the machine's case temperature continues to rise, finally reaching 109° C. When active, the MRAC and BEMF detector provide torque regulation with minimal additional software.

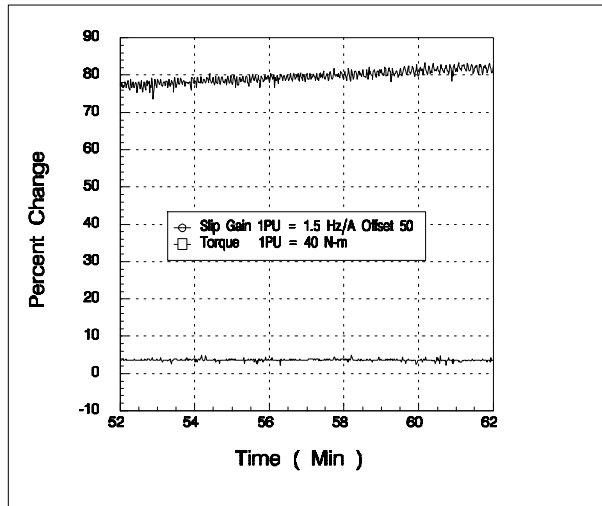
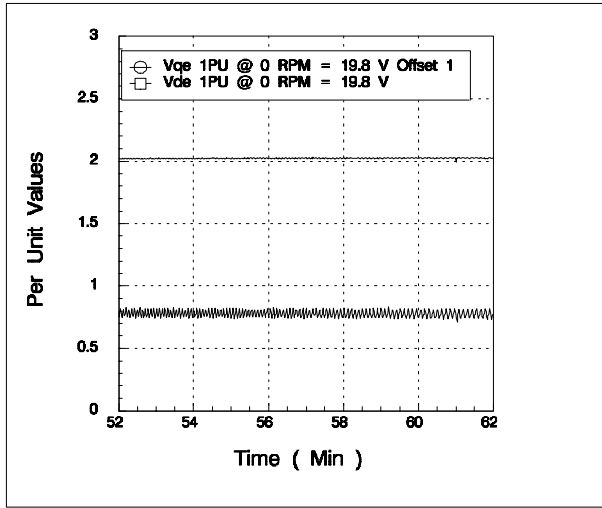


Fig. 12. Sensor IFOC with BEMF Detector of Fig. 8a. 8° C Rise - Experimental.

Fig. 12 shows results for the BEMF detector over an 8° C temperature rise. The torque remains constant and the slip gain increases, reflecting the change in rotor resistance. Thus the control's ability to correct for a small temperature variation is clearly demonstrated. With its ability to resolve small variations in the motor's resistances, the BEMF technique provides an accurate and rapid response controller for FO.

The excellent dynamic response of the BEMF configuration of Fig. 8a is not surprising given its location in the feedback loop. To establish the response of the configuration of Fig. 8b, tests were conducted with a selectable series resistance inserted between the drive and motor terminals. Fig. 13 is typical of the results obtained.

The drive control is a sensorless IFOC and the motor a 7.5 Hp, 4 pole, induction machine. The machine was

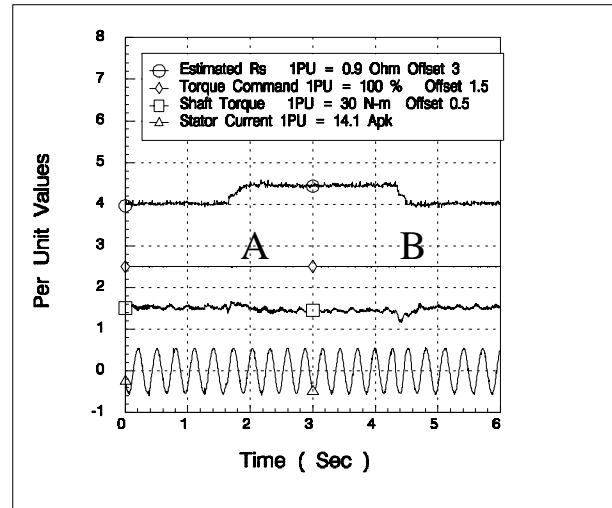


Fig. 13. Sensorless IFOC with BEMF Detector of Fig. 8b. Step change in Stator Resistance at 30 rpm Full Load - Experimental.

running at 30 rpm with rated torque applied. The top trace shows the estimate of the stator resistance as calculated by (14). The next three traces are the torque command, shaft torque, and stator current respectively. At point A, the stator resistance is increased approximately 50%. The BEMF detector responds rapidly with an estimate of the stator resistance and the torque is barely disturbed. At B, the inserted resistance is removed; again, the BEMF detector estimates the new resistance and supplies this estimate to the MRAC with a small disturbance in the torque. Although these are unlikely disturbances in practice, the tests do show a rapid convergence to the effective stator resistance; thus, the dynamic response of the BEMF is established.

## VI. CONCLUSION

An analysis of the effects of machine parameters on torque control showed the importance of an accurate estimate of the stator resistance. Time domain computer simulations and experimental results confirmed the steady state analysis. Through a simple analysis of a MRAC based rotor time constant estimator, an explanation was presented for the inherent difficulty accompanying the estimation of the feedback flux signal at low speed.

A new flux and stator resistance identifier was presented that provided an uncorrupted flux signal for purposes of adaptation. The BEMF detector resolves the feedback voltage into a new reference frame wherein one component presents a signal proportional to the axis flux and the quadrature component may be employed to estimate the stator flux. The proposed BEMF detector has at least two implementations; one is incorporated in the feedback loop, and the other is

employed as an observer to estimate the stator resistance for the standard MRAC.

Experimental results were presented showing the steady state and transient performance of the BEMF detector. The results showed the BEMF detector has excellent dynamic and transient characteristics, capable of resolving a 8° C case temperature change and responding to a step change in stator resistance with a small disturbance in the torque.

#### REFERENCES

- [1] Norbert R. Klaes, "Accurate Off-Line Identification of the Operating Point Dependent Induction Machine Parameters," EDS '90, Electrical Drives Symposium, Capri, 25-27 Sept. 1990.
- [2] M. Depenbrock and N. R. Klaes, "Determination of the Induction Machine Parameters and Their Dependencies on Saturation," in Conf. Rec. 1989 IEEE IAS Ann. Mtg., pt. I, pp. 17-22.
- [3] T. Okuyama, N. Fujimoto, T. Matsui, and Y. Kubota, "A High Performance Speed Control Scheme of Induction Motor Without Speed and Voltage Sensors," in Conf. Rec. 1986 IEEE IAS Ann. Mtg., pp. 106-111.
- [4] A. Boglietti, P. Ferraris, M. Pastorelli, C. Zimaglia, "Induction Motors Field Oriented Control Based on Averaged Parameters," in Conf. Rec. 1994 IEEE IAS Ann. Mtg., pp. 81-87.
- [5] T. M. Rowan, R. J. Kerkman, and D. Leggate, "A Simple On-Line Adaption for Indirect Field Orientation of an Induction Machine," IEEE Trans. on Industry Applications, Vol. 27, No. 4, July/August 1991, pp. 720-727.
- [6] R. D. Lorenz and D. B. Lawson, "A Simplified Approach to Continuous, On-line Tuning of Field-Oriented Induction Machine Drives," in Conf. Rec. 1988, pp. 444-449.
- [7] Thomas G. Habetler, Francesco Profumo, Giovanni Griva, Michele Pastorelli, and Alberto Bettini, "Stator Resistance Tuning in a Stator Flux Field Oriented Drive Using an Instantaneous Hybrid Flux Estimator," European Power Electronics Conference 1993, Brighton, England, pp. 101-107.
- [8] Toshiaki Okuyama, Noboru Fujimoto, and Hiroshi Fujii, "A Simplified Vector Control System without Speed and Voltage Sensors - Effect of Setting Errors of Control Parameters and Their Compensation," Electrical Engineering in Japan, Vol. 110, No. 4, 1990, pp. 129 - 139.
- [9] L. J. Garces, "Parameter Adaption for the Speed Controlled Static AC Drive with a Squirrel-Cage Induction Motor," IEEE Trans. on Industry Applications, Vol. IA-16, Mar./Apr. 1980, pp. 173-178.
- [10] G. Heinemann and W. Leonhard, "Self-tuning Field Oriented Control of an Induction Motor Drive," Proceedings of 1990 International Power Electronics Conference, Tokyo, April 2-6, 1990, pp. 465-472.
- [11] J. C. Moreira, K. T. Hung, T. A. Lipo, and R. D. Lorenz, "A Simple and Robust Adaptive Controller for Detuning Correction in Field Oriented Induction Machines," IEEE IAS Ann. Mtg., Sept. 28-Oct. 4, 1991, pp. 397-403.
- [12] Takafumi Maruyama and Hideto Negoro, "A Stator and Rotor Resistance Estimation Method Based on Motor Voltage Equations and Current Control Variables in Steady State," Proceedings of 1995 International Power Electronics Conference, IPEC-Yokohama '95, pp.1290-1295.